RASĀYAN *J. Chem.*
Vol. 17 | No. 3 |1290-1298| July - September | 2024
ISSN: 0974-1496 | e-ISSN: 0976-0083 | CODEN: RJCABP
http://www.rasayanjournal.com
http://www.rasayanjournal.co.in

SYNTHESIS, CHARACTERISATION, AND INVESTIGATION OF THERMAL AND ELECTROCHEMICAL PROPERTIES OF A NOVEL SALICYLAMIDE COORDINATED HIGH VALENT COBALT COMPOUND

S. Priyadarshini[1], G. S. Brahma[2], A. K. Sahu[2] and Suprava Nayak[1,✉]
[1]School of Chemistry, Gangadhar Meher University, Sambalpur-768004 (Odisha) India.
[2]Faculty of Science and Technology (IcfaiTech), The ICFAI Foundation for Higher Education, Hyderabad-501203, (Telangana) India.
✉Corresponding Author: suprava7107@gmail.com

ABSTRACT

A novel dimeric Cobalt compound, $[Co^{III}(L)(\mu\text{-}OH)]_2$. H_2O of ligand 1,3-propylene-bis(salicylamide) (H_2L) has been synthesized. XRD, FTIR and ^1H NMR were used to elucidate the structure of the complex. Elemental analysis (CHNS) and TGA were employed to find out the composition. Thermal analysis shows that the average specific heat capacity (Cp) of the complex is 1.86 J/gK. The redox potential of the complex has been established by cyclovoltammetry and it shows a quasi-reversible nature of the Co^{3+}/Co^{2+} couple. The optical bandgap (Eg) and refractive index of the complex were found to be 2.31 eV and 2.6 respectively. Thermal analysis revealed the thermal stability of the complex.

Keywords: Co(III) Coordination Compound, 1,3-propylene bis(salicylamide), Redox-Active, Heat-Dissipation, Specific Heat Capacity.

RASĀYAN *J. Chem.*, Vol. 17, No.3, 2024

INTRODUCTION

Design and synthesis of various metal organic motifs and embedding them into energy storage devices have attracted the attention of many researchers in recent years.[1-9] The denticity, type of donor atoms, and organic spacer unit of a ligand scaffold influences the usefulness of metal-organic complexes. Many works have been reported pertaining to metal-amide complexes such as metal-salicylamide[10-12], oxalamide[13], and thioglycolamide[14] due to their extensive applications in different fields such as developing synthetic polymers for storing gas, luminance, and magnetic applications, etc. This has become imminent because such complexes possess flexible spacer units between the amine and amide functional groups that give structural diversity as well and the aromatic carboxamide with hard N and O donor atoms provides a strong coordination with high valent metal ions. Salicylamide ligands can be highly effective for constructing multinuclear metal clusters owing to their coordinating ability through phenolate-O, and amide-N. In addition, they can be accessed from cheap and available raw materials. Earlier a high valent binuclear iron complex with phenolate-amide-amine coordinating ligand has been reported by us.[15] This field offers numerous combinations of metal ions and organic linker molecules for exploration. Therefore, it is always worthwhile to study the properties of newly developed compounds. It is found that not much research has been done on metal-salicylamide compounds for heat storage. In this work, we have synthesized a salicylamide-based dimeric cobalt(III) compound, $[Co^{III}(L)(\mu\text{-}OH)]_2$ (see Scheme-1), and studied its properties which have not been reported earlier.

EXPERIMENTAL

Material and Methods

Double-distilled water was used to prepare all of the solutions, the second distillation was made from alkaline $KMnO_4$, and an all-glass distillation apparatus was used for this. All chemicals used were of analytical grade. The reagents methyl salicylate, and (1,3)-diaminopropane, (SRL) were, used for the synthesis of ligands. The reagents $CoCl_2$, $6H_2O$ (BDH, AR), LiOH, and H_2O (AR) were used for the synthesis of a dimeric Co complex $[Co^{III}(L)(\mu\text{-}OH)]_2$.

http://doi.org/10.31788/RJC.2024.1738894

Instrumentation

Thermo-Nicolet Nexus 670 setup in the 400–4000 cm^{-1} range was used to identify the functional groups from FTIR data analysis. ^1H NMR of the complex was taken in a Bruker Avance III (400 MHz) instrument. Using Cu K-alpha radiation (wavelength = 1.5406 Å), an X-ray diffraction study was conducted on a PAN analytical Empyrean X-ray diffractometer. The 2θ range of 10^0 to 80^0 is used, with each step having an acquisition time of one second and a step size of 0.01^0. The crystallite size was determined from the full width at half maximum of their XRD peaks. The X' Pert High Score Plus software was used to evaluate the X-Ray diffraction pattern. The band gap (Eg) of the complex was determined with the help of UV-Vis-NIR analysis (Varian Cary 5000 spectrophotometer) and this analysis was conducted in the wavelength range 200 to 2500 nm at room temperature. The CHN analysis was performed using Thermoscientific Flash EA 1112 (elemental analyzer). With a heating rate of 10 K/min, the specific heat capacity of the synthesized cobalt complex was determined using differential scanning calorimetry (DSC Discovery 250 equipment). All DSC measurements were carried out in the aluminum crucible between the temperature range of 30 to 250°C in a normal atmosphere.

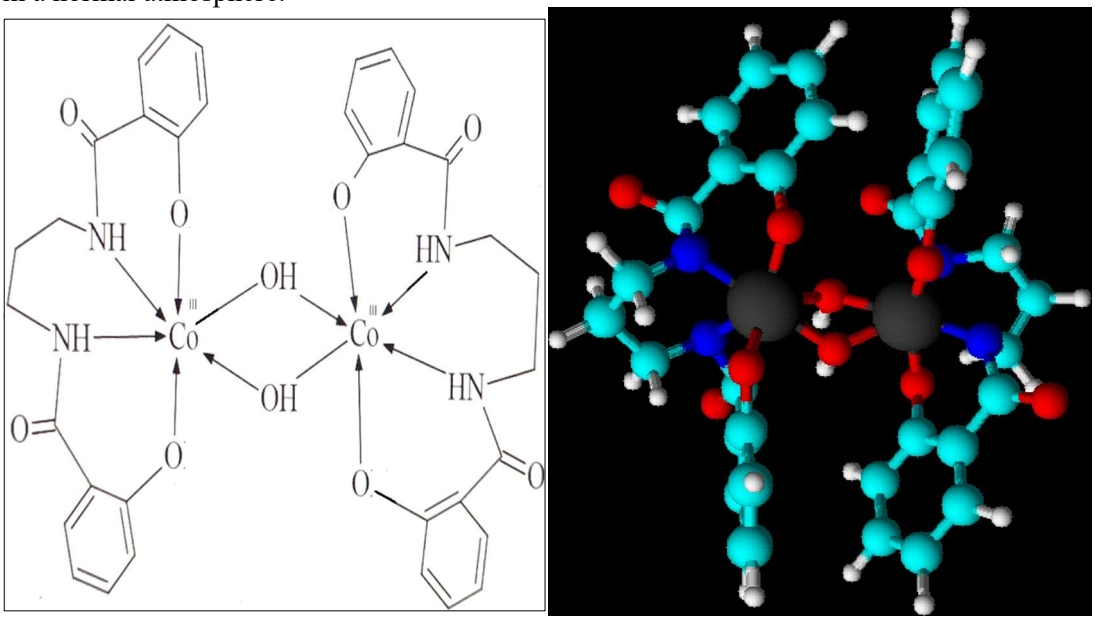

(a) (b)

Scheme-1: Structure of the Cobalt Complex $[Co^{III}(L)(\mu\text{-}OH)]_2$ (a) 2D Structure and (b) 3D-Optimized Structure

Thermogravimetric analysis (TGA), Derivative thermogravimetry (DTG), and Thermal decomposition studies were done in the temperature range of 40 to 500°C on a TAQ600 thermal analyzer in a normal atmosphere using an aluminum crucible. These analyses were all carried out at STIC-Cochin. Cyclovoltammetry was run at 0.1V/s scan rate with 3mm diameter glassy carbon as a working electrode at NIT Rourkela, Odisha.

Synthesis of Ligand (H_2L)

The method of preparation of ligand (1,3)bis(2-hydroxybenzamido)propane (H_2L) was adopted from our earlier paper.[16] The ligand H_2L was synthesized by combining methyl salicylate with 1,3-diammino propane in a beaker at a 2:1 ratio while stirring. The mixture was then digested and concentrated for five to six hours at water bath temperature. The crude product is obtained as a thick viscous mass and it is recrystallized from 50% MeOH + H_2O and stored over silica gel in a desiccator. The FTIR data obtained for the ligand was similar to our previously published findings.[16]

Synthesis of Complex $[Co^{III}(L)(\mu\text{-}OH)]_2.H_2O$

An aqueous solution of $CoCl_2.6H_2O$ (0.01 mol) was added dropwise to the 1: 2 molar mixture of ligand(L) (0.01 mol) and LiOH (0.02 mol) in warm methanolic solution while stirring. The colorless ligand solution progressively became bluish violet upon the addition of a small quantity of $CoCl_2$ solution. When all the

$CoCl_2$ solution was added, the color deepened and became violet precipitate. The violet precipitate changed into a dark green precipitated solution upon raising the pH by addition of extra 0.01 mol of LiOH solution. The resulting solution was agitated by a magnetic stirrer for 5-6 hours. The solution was allowed to undergo aerial oxidation for 3-4 days and then heated at around 100 °C for 1-2 days and a reddish pink colored solution was obtained below the green precipitate. It was filtered off, and the reddish-pink-colored filtrate was collected. The pictorial representation of the synthesis of the cobalt complex is shown below (Scheme-2). The volume of the solution was reduced to half in a water bath at (50 - 60 °C). The resulting solution was set aside for slow evaporation, till all aqueous portions were exhausted and the pink-colored solid crystalline mass was isolated. The yield of the complex is 35%. Anal. calcd. for complex $C_{34}H_{36}Co_2N_4O_{11}$ is C(51.40), H(4.57), N (7.05) and Co(14.83) % ; Found C(51.12), H(4.66), and N(7.95) and Co(15.18) %. This elemental analysis is in agreement with the molecular formula of the complex $[Co^{III}(L)(\mu\text{-}OH)]_2.H_2O$.

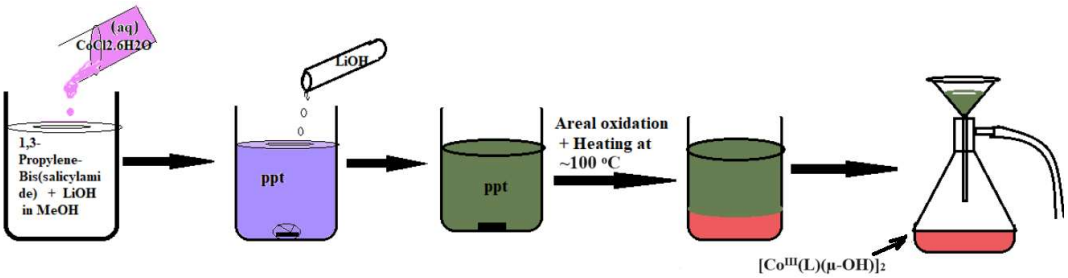

Scheme-2: Pictorial Representation of the Synthesis of Cobalt Complex, $[Co^{III}(L)(\mu\text{-}OH)]_2$

RESULTS AND DISCUSSION

FTIR Spectroscopic Study

Figure-1 shows the FTIR spectrum of the complex, $[Co^{III}(L)(\mu\text{-}OH)]_2$. A sharp with medium-intensity peak at 3373 cm^{-1} due to amide N-H stretching. The peak at 1643 cm^{-1} is for amide(νC=O) and peaks at 1591 and 1545 are for amide-II [νC-N + δ N-H]. Phenyl ring vibrations could be the cause of the absorption bands near 1452–1477 cm^{-1}, 1045–1069 cm^{-1} and 720–752 cm^{-1}. Most importantly, the bridged μ-O-H stretch has been identified at 3567 cm^{-1}, which is in tune with the result published for the bis-(μ-hydroxo) diiron(III) complex.[17] The IR band at ~ 915 cm^{-1} which has been assigned to a $Co(OH)_2Co$ deformation mode is in agreement with the observations made with analogous hydroxo-bridged complexes.[18] Further, the intense and sharp band at 518 cm^{-1} is due to the Co-OH-Co stretching vibration of the bi-nuclear cobalt complex. Similar findings on hydroxo-bridged Cr, Co, Cu, and Pt complexes have been previously reported, wherein asymmetric M-OH-M vibrations were found at 480-580 cm^{-1}.[19,20]

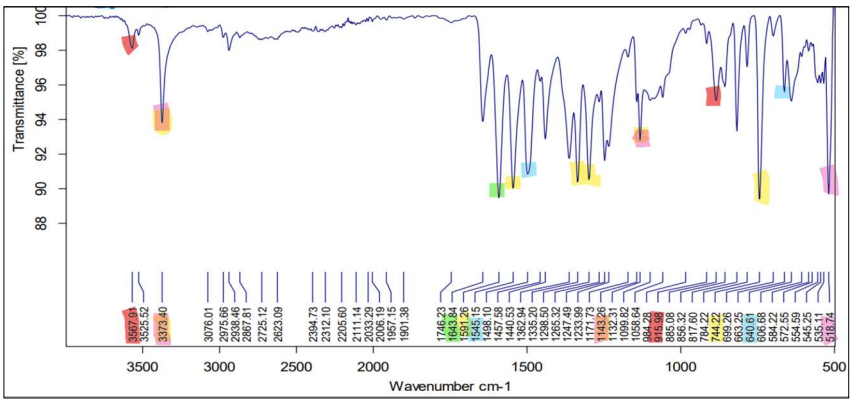

Fig.-1: FTIR Spectrum of the Cobalt Complex $[Co^{III}(L)(\mu\text{-}OH)]_2$

X-Ray Diffraction (XRD) Study

The XRD pattern of Complex $[Co^{III}(L)(\mu\text{-}OH)]_2$ is shown in Fig.-2. The diffraction patterns of the complex molecules that are made up of metal salt, cobalt chloride hexahydrate $CoCl_2 \cdot 6H_2O$, ligand 1,3-propylene-bis(salicylamide) is in good agreement with the published literature of Sheldrick *et.al*.[21] The complete analysis of the X-ray diffraction pattern was done and the results are exemplified in Table-1.

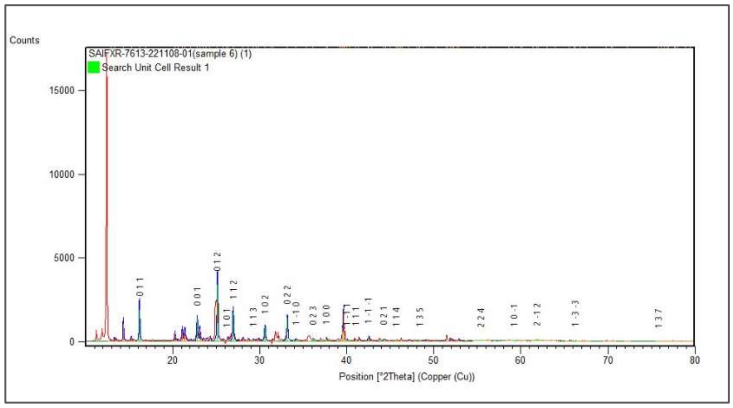

Fig.-2: XRD Pattern of Complex $[Co^{III}(L)(\mu\text{-}OH)]_2$

Table-1: XRD Parameters of the Complex

S.No.	Parameter	Value
1.	*Cell candidates*	
	a	3.7362 Å
	b	5.8129 Å
	c	9.8754 Å
	α	36.4764^0
	β	49.5637^0
	δ	74.0565^0
	Cell volume	81.3325 $Å^3$
2.	Crystal system	Triclinic
3.	Bravias type	Primitive (P)
4.	Space Group	P 1

Determination of the Size of Crystallites

Equation (1) is used to compute the crystallite size of the complex using the classical Debye-Scherrer equation as shown below:

$$d = \frac{K \times \lambda}{\beta \times \cos\theta} \qquad (1)$$

Where K is the dimensionless shape factor (0.9), the wavelength of Cu-kα radiation is λ (1.54065 Å), θ is half of the Bragg's diffraction angle of the most intense peak, and β is taken as full-width at half maximum (FWHM). The average crystallite size is found to be 105.6nm which is determined from the plot shown in Fig.-3 as well as by using the method of Williamson and Hall.[22] XRD data indicate the complex is 70% crystalline.

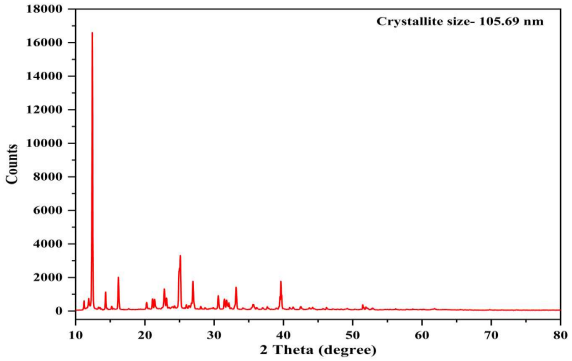

Fig.-3: Determination of Crystallite Size from XRD Graph of $[Co^{III}(L)(\mu\text{-}OH)]_2$ Complex

UV-Visible Spectroscopic Study

The UV-visible spectrum of the $[Co^{III}(L)(\mu\text{-}OH)]_2$ complexes in a wavelength range of 200 nm to 700 nm is displayed in Fig.-4. The absorption maxima, λ_{max} of the complex arises at 537 nm and a shoulder appears at 485 nm. These bands are due to ligand-to-metal charge transfer (LMCT) i.e. from ligand sigma orbital

to the metal t_{2g} molecular orbital. The calculated bandgap and refractive index from the absorption maxima of the complex are found to be 2.32 eV and 2.6 respectively.

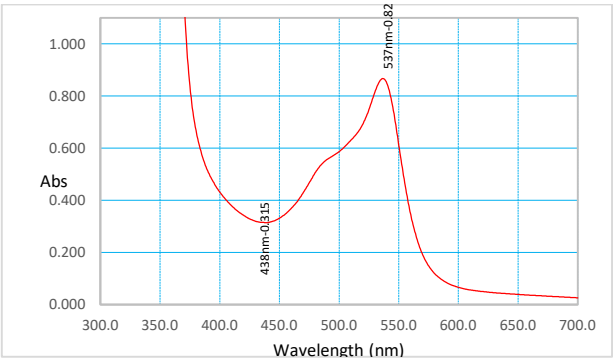

Fig.-4: UV-Visible Spectrum of Complex $[Co^{III}(L)(\mu\text{-}OH)]_2$ of Concentration 1.4 x 10^{-4} mol dm^{-3} in Aqueous Medium

^{1}H NMR Spectroscopic Study

No Phenolic proton peak in the 1H NMR spectrum of the complex (Fig.-5) further indicates the coordination of deprotonated phenoxide O to the Co^{III} center. In the aromatic region, the proton H_d and H_b exhibit doublet and triplet peaks at around δ 7.79 and δ 7.35 respectively, whereas the doublet of H_a and triplet of H_c peaks coincide sufficiently to appear as a multiple at around δ 6.85. With respect to the peak for aliphatic protons in the spacer propylene group, two H_f protons of the center CH_2 group yield a pentate at δ 1.93 while two side CH_2 groups (four H_e protons) that are next to the amide group give a triplet at δ 3.5.

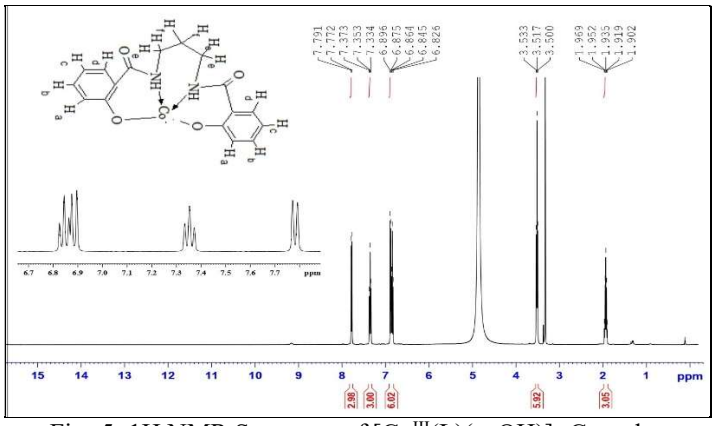

Fig.-5: 1H NMR Spectrum of $[Co^{III}(L)(\mu\text{-}OH)]_2$ Complex

Differential Scanning Calorimetry, (DSC)

DSC study (heating and cooling) was performed on the complex with a heating rate of 10K/min to examine its thermal behavior. Heat flow curves and specific heat capacity of $[Co^{III}(L)(\mu\text{-}OH)]_2$ complex in a temperature range of 30 °C to 250 °C are shown in Fig.-6 and Fig.-7 respectively. Figure-6 depicts the DSC thermogram of the titled complex. From the thermogram, it is found that the material showed endothermic behavior in the first heating cycle by a sharp peak (down) from 88.12K to 100.54K and from 141.10K to 182.53K which corresponds to the loss of one coordinated water molecule. During cooling, it showed exothermic behavior in the entire cycle. The second heating cycle exhibited the glass transition step from 38.16K to 49.45K with the center point at 43.89K, and the material exhibited predominantly exothermic behavior. Owing to the exothermic property of the material, the complex, $[Co^{III}(L)(\mu\text{-}OH)]_2$ can be considered as heat-dissipating material.[23] Glass transition was observed at 43.01 °C from 2nd heating which can be confirmed from the cooling segment. The integral normalized peak was observed at 95.83 °C. From the heat flow curve (Fig.-6) we can see the plot of the 1st heating, 2nd heating, and cooling segments also. The observed average specific heat capacity of the complex is 1.86 J/gK. Hence, the DSC study revealed that the phase change of the complex is endothermic in nature. Figure-7 shows the thermal cycle of specific heat capacity versus temperature plot at the range of 30 °C to 250 °C for complex material.

Thermogravimetric Study

The thermogravimetric (TG) properties of the synthesized $[Co^{III}(L)(\mu\text{-}OH)]_2.H_2O$ complexes were investigated and are exemplified in Fig.-8. In the complex, the phase in the range of 40-500 ºC should concern the decomposition of the complex non-coordinated H_2O molecule released at 120 ºC with a weight loss of 2.8% (calc. 2.26%). The plot indicates dehydrated cobalt complex further undergoes decomposition at 280 ºC and continues till 330 ºC with a weight loss of around 80%. This large loss of weight is attributed to the loss of coordinated ligand molecules from the complex which further confirms the composition of the complex with one water molecule present as water of crystallization. In the range of 40 ºC to 500 ºC, from the DTG curve of the complex two decomposition processes, at 130 and 320 ºC were detected. The TG-DTA graph of the complex indicates the endothermic dissociation of the dehydrated complex commencing at 280ºC and continuing till 330ºC, and finally leaving behind the metal oxide.

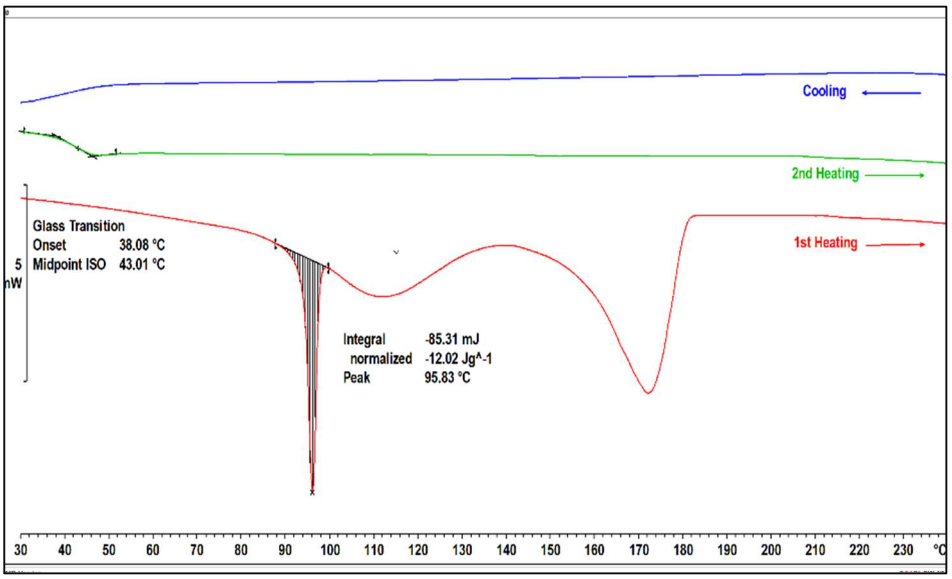

Fig.-6: DSC, Heat Flow Curves of $[Co^{III}(L)(\mu\text{-}OH)]_2$ Complex

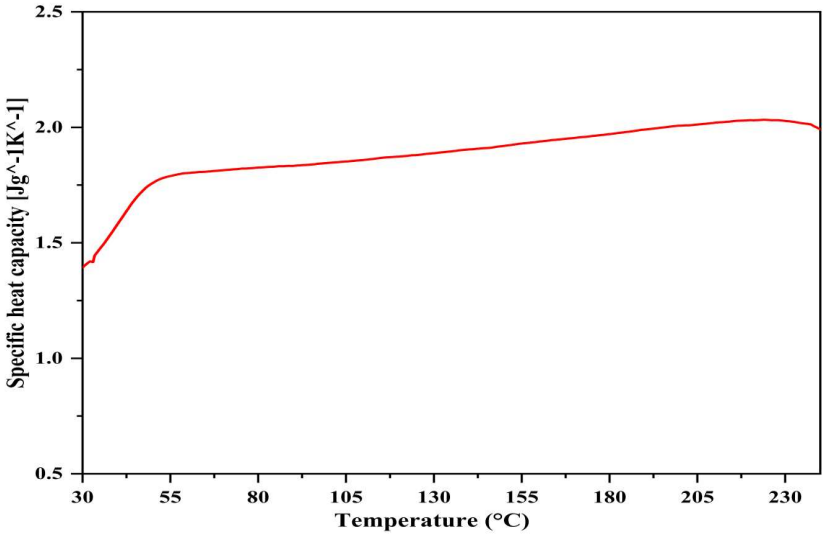

Fig.-7: Specific Heat Curve of $[Co^{III}(L)(\mu\text{-}OH)]_2$ Complex

Cyclovoltammetry Study

Cyclic Voltammetry was run at a 2.0V/s scan rate with 3mm diameter glassy carbon as the working electrode, Ag/AgCl as reference, and platinum wire as counter electrodes. The electrolyte was 60% methanol and the concentration of analyte was 1mM. Two peaks in the cathodic region at 485mV and -42mV and at the anodic region one peak at 109mV were found (Fig.-9a).

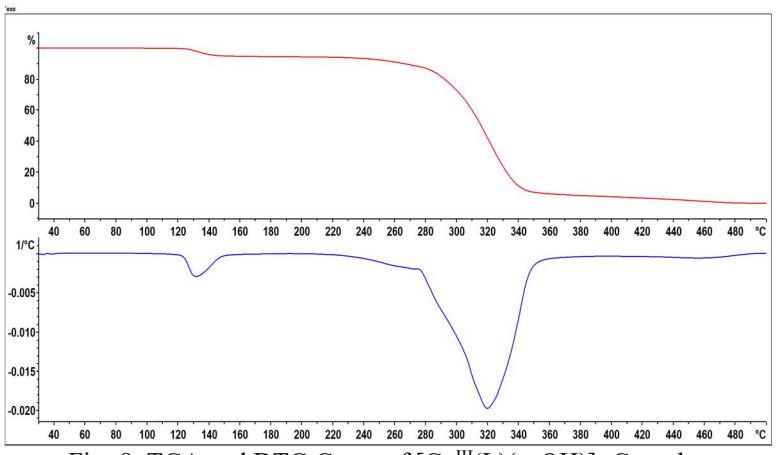

Fig.-8: TGA and DTG Curve of $[Co^{III}(L)(\mu\text{-}OH)]_2$ Complex

To enhance reproducibility, the voltammogram was also obtained at a 0.1 V/s scan rate. Two peaks in the cathodic region at 178mV and 580mV and at the anodic region no peak was found (Fig.-9b). The disappearance of the peak in the anodic region at a slow scanning rate is owing to the elongation of the shoulder of the anodic peak otherwise visible at higher voltage ramping conditions. No evidence of any further electron exchange was observed in the oxidation half cycle. This characteristic enunciates the quasi-reversible nature of the Co^{3+}/Co^{2+} couple, exhibited in the electrochemical window, is due to the inherent reducing tendency of the associated ligand, L, evidently electrochemical profiles largely tuned by the Co^{3+} species in an octahedral environment.[24]

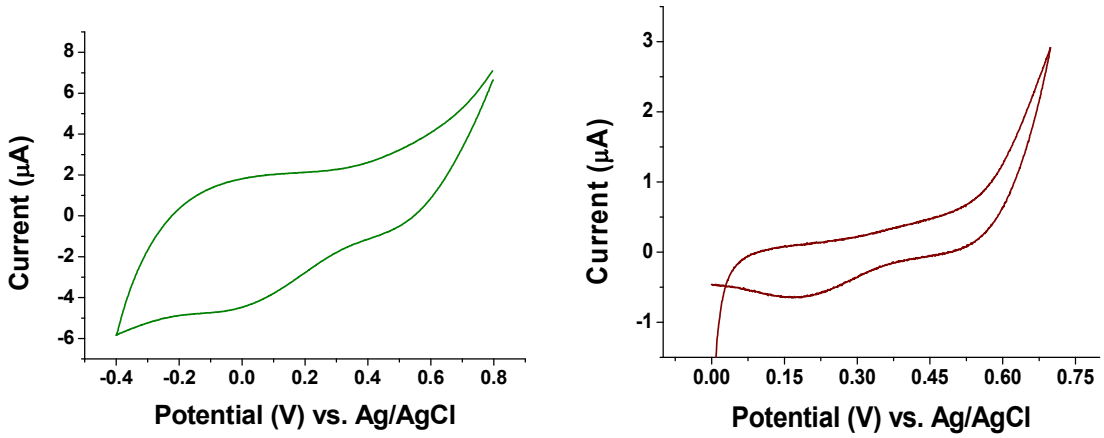

(a) (b)

Fig.-9: Cyclic Voltammograms of $[Co^{III}(L)(\mu\text{-}OH)]_2$ in Methanol with concentration of Complex 1.0×10^{-4} mol dm^{-3} with Scan Rate (a) 2.0V/s and (b) 0.1V/s

CONCLUSION

A high valent and water-soluble dimeric Cobalt complex $[Co^{III}(L)(\mu\text{-}OH)]_2$ was obtained by reacting the ligand 1,3-propylene bis(salicylamide) (H_2L) with cobalt chloride hexahydrate at a high pH reaction condition, followed by areal oxidation and heating. This reddish-pink-colored complex displays LMCT transitions with a high extinction coefficient (3875 L mol^{-1} cm^{-1}) at 537 nm. The synthesized complex is 70% crystalline with an average crystallite size of 105.6nm. The quasi-reversible nature of the Co^{3+}/Co^{2+} couple exhibited in the electrochemical window, is due to the inherent reducing tendency of the associated ligand, L. DSC study revealed that the phase change of the complex is endothermic in nature but overall $[Co^{III}(L)(\mu\text{-}OH)]_2$ can be considered as heat-dissipating material.

ACKNOWLEDGMENTS

Dr. Suprava Nayak (SN), acknowledges the OURIIP Seed Fund (Grant Index number: OURIIP-2020/ 37/Chemistry), Odisha State Higher Education Council, Government of Odisha, India, for financial

assistance. The author SP is grateful to G.M. University, Sambalpur, Odisha for providing the necessary facilities to carry out this work. GSB and AKS are grateful to the Faculty of Science and Technology (IcfaiTech), and IFHE for providing the necessary support to get associated with this work.

CONFLICT OF INTERESTS

The authors certify that there is no conflict of interest associated with the publication of this article.

AUTHOR CONTRIBUTIONS

All the authors contributed significantly to this manuscript, participated in reviewing/editing, and approved the final draft for publication. The research profile of the authors can be verified from their ORCID IDs, given below:

S. Priyadarshini http://orcid.org/0000-0002-4595-1577
G.S.Brahma https://orcid.org/0000-0001-5380-983X
A.K. Sahu http://orcid.org/0000-0002-6272-7809
Suprava Nayak http://orcid.org/0000-0002-4872-2665

REFERENCES

1. N.O. Laschuk, I. I. Ebralidze, E. B. Easton and O. V. Zenkina, *ACS Applied Energy Materials*, **4(4)**, 3469(2021), https://doi.org/10.1021/acsaem.0c03218
2. J. W. Gittins, C. J. Balhatchet, S. M. Fairclough and A. C. Forse, *Chemical Science*, **13(32)**, 9210(2022), https://doi.org/10.1039/D2SC03389E
3. B. Zhu, D. Wen, Z. Liang and R. Zou, *Coordination Chemistry Review*, **446**, 214119(2021), https://doi.org/10.1016/j.ccr.2021.214119
4. K. W. Nam, S. S. Park, R. dos Reis, V. P. Dravid, H. Kim, C. A. Mirkin and J. F. Stoddart, *Nature Communication*, **10,** 4948(2019), https://doi.org/10.1038/s41467-019-12857-4
5. Y. Chen, Q. Zhu, K. Fan, Y. Gu, M. Sun, Z. Li, C. Zhang, Y. Wu, Q. Wang, S. Xu, J. Ma, C. Wang and W. Hu, *Angewandte Chemie International Edition*, **60**, 18769(2021), https://doi.org/10.1002/anie.202106055
6. S. Gu, Z. Bai, S. Majumder, B. Huang and G. Chen, *Journal of Power Sources*, **429**, 22(2019), https://doi.org/10.1016/j.jpowsour.2019.04.087
7. Z. Wu, D. Adekoya, X. Huang, M. J. Kiefel, J. Xie, W. Xu, Q. Zhang, D. Zhu and S. Zhang, *ACS Nano*, **14(9)**, 12016(2020), https://doi.org/10.1021/acsnano.0c05200
8. J. Liu, X. Song, T. Zhang, S. Liu, H. Wen and L. Chen, *Angewandte Chemie International Edition*, **60**(11), 5612(2021), https://doi.org/10.1002/anie.202006102
9. K. B. Wang, Q. Xun and Q. Zhang, *EnergyChem*, **2(1)**, 100025(2020), https://doi.org/10.1016/j.enchem.2019.100025
10. H. Phetmung and A. Nucharoen, *Polyhedron*, **173**, 114121(2019), https://doi.org/10.1016/j.poly.2019.114121
11. M. Koikawa , H. Maeda , H. Ōkawa , N. Matsumoto ,S. Kida , K. Inamoto and T. Tokii, *Synthesis and Reactivity in Inorganic and Metal-Organic Chemistry*, **25**:9, 1479(1995), https://doi.org/10.1080/15533179508218284
12. X. Song, L. Wang, M. Zhao, G. Cheng, X. Wang, Y. Peng, *Inorganica Chimica Acta*, **402**, 156(2013), https://doi.org/10.1016/j.ica.2013.03.040
13. V. A. Mamedov, V. L. Mamedova, V.V. Syakaev, T.A. Kushatov, D. E. Korshin, I. K.Rizvanov, A. T. Gubaidullin; *Tetrahedron*,**150**, 133751(2024), https://doi.org/10.1016/j.tet.2023.133751
14. J. Singh, R. Kanaoujiya, A. Jaiswal, A. Pal, Meenakshi and S. Srivastava, *Rasayan Journal of Chemistry*, **16**, 2, 839(2023), http://doi.org/10.31788/RJC.2023.1618254

15. S. Nayak and A. C. Dash, *Transition Metal Chemistry*, **31**, 813(2006), https://doi.org/10.1007/s11243-006-0079-0
16. S. Nayak and A. C. Dash, *Indian Journal of Chemistry,* **42A,** 2427(2003), http://nopr.niscpr.res.in/handle/123456789/20797
17. J.A. Thich, C. C. Ou, D. Powers, B. Vasiliou, D. Mastropaolo, J. A. Potenza.and H. J. Schugar, *Journal of the American Chemical Society*, **98**, 1425(1976), https://doi.org/10.1021/ja00422a024
18. D. M. Kurtz. Jr., *Chemical Reviews,* 90, 585(1990), https://doi.org/10.1021/cr00102a002
19. (a) D. J. Hewkin, and W. P. Griffith, *Journal of the Chemical Society A: Inorganic, Physical, Theoretical*, 472(1966), https://doi.org/10.1039/J19660000472 ; (b) W. R. McWhinnie, *Journal of Inorganic and Nuclear Chemistry,* **27**, 1063(1965)
20. (a)G. Blyholder, N. Ford, *Journal of Physical Chemistry,* **68**, 1496(1964), https://doi.org/10.1021/j100788a039 (b) J. R. Ferraro; W. R. Walker, *Inorganic Chemistry*, **4**, 1382(1965), https://doi.org/10.1021/ic50032a002
21. G. M. Sheldrick, *Acta Crystallographica Section A: Foundations and Advances*, **71(1)**, 3(2015), https://doi.org/10.1107/S2053273314026370
22. G. K. Williamson and W.H. Hall, *Acta Metallurgica*, **1**, 22(1953), https://doi.org/10.1016/0001-6160(53)90006-6
23. Y. Oba and T. Mochida, *Polyhedron*, 99, 275((2015), https://doi.org/10.1016/j.poly.2015.08.015
24. A. Murugkar, R. Bendre, A. Kumbhar and S. Padhye, *Indian Journal of Chemistry-A*, **38A**, 977(1999).

[RJC-8894/2024]